Crystallization of phosphatidylinositol-specific phospholipase C from *Bacillus cereus*

Timothy L. Bullock, Margret Ryan, Suezane L. Kim, S. James Remington, and O. Hayes Griffith
Institute of Molecular Biology, University of Oregon, Eugene, Oregon 97403 USA

ABSTRACT Phosphatidylinositol-specific phospholipase C (PI-PLC) cleaves phosphoinositides into two parts, lipid-soluble diacylglycerol and the water-soluble phosphorylated inositol. Two crystal forms of *Bacillus cereus* PI-PLC have been obtained by the vapor diffusion technique. Hexagonal crystals were grown from solutions containing polyethylene glycol (PEG; 4,000 to 8,000 D). The space group of these hexagonal crystals is $P6_122$ (or the enantiomorphic space group $P6_522$), with cell constants $a = b = 133$ Å, and $c = 231$ Å. The crystals diffract to 2.8 Å. The second crystalline form was grown from a two-phase PEG (600 D)–sodium citrate solution. The phase diagram and PI-PLC distribution between phases has been determined. The enzyme crystallizes from the PEG-rich phase. The crystals are orthorhombic with space group $P2_12_12_1$ ($a = 45$ Å, $b = 46$ Å, $c = 160$ Å), and contain one PI-PLC monomer per asymmetric unit. The orthorhombic crystals diffract to 2.5 Å. Both the hexagonal and orthorhombic forms are suitable for crystallographic studies.

INTRODUCTION

Phosphatidylinositol-specific phospholipase C (PI-PLC) (EC 3.1.4.10) cleaves phosphoinositides into two parts: the lipid-soluble diacylglycerol, and the phosphorylated water-soluble inositol headgroup. An increasing number of PI-PLCs are being found in both eukaryotes and prokaryotes. They are secreted by a variety of bacteria, including *Bacillus cereus* (1, 2) and the closely related *Bacillus thuringiensis* (3, 4), the human pathogens *Staphylococcus aureus* (5) and *Listeria monocytogenes* (6–8), and the marine bacterium *Cytophaga sp.* (NCMB 1314, 9). PI-PLC is one of three classes of enzymes that have phospholipase C activity. Another type is phosphatidylcholine-hydrolyzing phospholipase C (PC-PLC, sometimes called lecithinase). PC-PLC is less specific, hydrolyzing phosphatidylcholine, phosphatidylethanolamine, and phosphatidylserine. The crystal structure of a phosphatidylcholine-hydrolyzing phospholipase from *B. cereus* has been reported (10). A third enzyme with a phospholipase C-like activity is sphingomyelinase. These latter two enzymes do not hydrolyze PI. There appears to be little or no sequence homology between these three types of phospholipases C.

The bacterial PI-PLCs also cleave glycosylphosphatidylinositol (GPI), a derivative of PI, and thus release GPI-anchored proteins from membrane surfaces (11). The parasitic protozoan *Trypanosoma brucei* has a GPI-PLC thought to play a role in the ability of trypanosomes to shed the variable surface glycoprotein (12–15). The malaria-causing *Plasmodium falciparum* evidently has a PI-PLC activity (16, 17), as has the cellular slime mould *Dictyostelium discoideum* (18).

In higher eukaryotes, PI-PLCs are involved in signal transduction. *Drosophila* PI-PLCs have been reported (19–21), and an avian PI-PLC from turkey erythrocytes has been sequenced (22, 23). Mammalian PI-PLCs have been found in nearly all tissues examined (for reviews see 24–26). In some mammalian cells in culture, PI-PLC activity is also present on the exterior surface (27, 28). In addition, PI-PLCs are being reported in higher plants (29, 30).

The purpose of this paper is to report the successful crystallization of a member of the PI-PLC family of enzymes. We selected the *B. cereus* PI-PLC because it is a relatively small enzyme (35 kD) compared to the PI-PLCs of higher eukaryotes (85–155 kD). Also, the *B. cereus* PI-PLC has been overexpressed in *E. coli* so that sufficient quantities are available for x-ray crystallography studies (31).

MATERIALS AND METHODS

Chemicals and biochemicals

Polyethylene glycol of average molecular weight 600 (PEG 600; Sigma Chemical Co., St. Louis, MO), sodium citrate dihydrate ("Baker Analyzed" grade; J. T. Baker Inc., Phillipsburg, NJ), HEPES (free acid; Calbiochem, La Jolla, CA) and *myo*-inositol (Aldrich Chemical Co., Milwaukee, WI; and Sigma Chemical Co., St. Louis, MO) were used without further purification. Precipitant solutions for growing orthorhombic crystals, as well as total systems used to determine the phase diagram and PI-PLC partitioning, were prepared from the following stock solutions: 1 M and 1.6 M sodium citrate dihydrate, pH to 7.3 with HCl; 1 M HEPES, pH to 7.9 with NaOH; 0.5 M *myo*-inositol. These solutions were sterilized using cellulose acetate membrane filters (0.2 μm pore size; Nalgene; Nalge Company, Rochester, NY; or Uniflow-25; Schleicher & Schuell, Inc., Keene, NH) and stored in sterile polypropylene tubes (50 ml capacity) at room temperature. Recombinant *B. cereus* PI-PLC was isolated from *E. coli* strain MM294 harboring the overexpressing plasmid pIC (31). The protein was stored in 20 mM Tris-HCl, pH 8.5, at −20°C. All aqueous solutions were prepared using sterile filtered deionized water. All our preparations contain no stabilizing or antimicrobial agents.

Crystallization

The *B. cereus* PI-PLC used for crystallization was transferred from 20 mM Tris-HCl, pH 8.5, to water by repeated ultrafiltration (Centricon-10; Amicon, Inc., Beverly, MA). The PI-PLC concentration in water was usually 6–8 mg/ml. All crystallization experiments were carried

Address correspondence to Dr. O. Hayes Griffith, Institute of Molecular Biology, University of Oregon, Eugene, OR 97403-1229, USA.

0006-3495/93/03/784/08 $2.00

out by vapor diffusion in hanging drops (32). Hanging drops were prepared by mixing 2–10 μl of protein with an equal volume of precipitant solution on glass cover slips (No. 2, round, 22 mm; VWR Scientific, Inc., Media, PA) which had been treated with siliconizing solution (AquaSil; Pierce, Rockford, IL/or Prosil-28; PCR Inc., Gainesville, FL). These cover slips were inverted and sealed over 1 ml of hypertonic reservoir solution (either precipitant or sodium chloride solution) in 24-well Linbro plates (Cat. No. 76-033-05; Flow Laboratories, McLean, VA).

Hexagonal crystals. Initially, in a screen of conditions using PEG as precipitating agent, hexagonal microcrystals formed in the presence of 5% (wt/vol) PEG 8000, 50 mM Tris-HCl, pH 7. Further crystallization trials were conducted using the sparse matrix sampling approach of Jancarik and Kim (33). Forty six of the fifty trial conditions of these authors were carried out, with one modification: the respective solutions were diluted 1:1 with water. Four sets of conditions yielded hexagonal crystals: (*a*) 0.1 M magnesium chloride, 50 mM Tris-HCl, pH 8.5, and 15% PEG 8000; (*b*) 0.1 M ammonium sulfate, 50 mM cacodylate, pH 6.5, and 15% PEG 8000; (*c*) 0.1 M sodium acetate, 50 mM Tris-HCl, pH 8.5, and 15% PEG 4000; and (*d*) 0.1 M ammonium sulfate, and 15% PEG 8000, pH 6.3 (unadjusted). These trials yielded no additional crystal morphologies. We experienced some difficulty in reproducing these crystals. However, by varying the growing conditions, crystals were almost always obtainable. The largest crystals grew in the presence of 15% PEG 4000, 0.15 M sodium acetate, and 0.1 M Tris-HCl, pH 8.5.

Orthorhombic crystals. The first orthorhombic crystals of *B. cereus* PI-PLC were grown at 4°C in the presence of 0.2 M sodium citrate, pH 5.6 and 45% PEG 600. This set of conditions gave small twinned crystals overnight. By changing the precipitant solution to 0.3 M sodium citrate, 28% PEG 600, 50 mM *myo*-inositol and 10 to 100 mM HEPES, pH 7.9, we have produced the larger single rods with a rectangular cross-section discussed below. Crystallization drops typically consisted of 10 μl protein solution mixed with 10 μl precipitant solution suspended over a reservoir of precipitant solution. Most drops gave hundreds of small crystals or no crystals at all. In order to find the optimal hypertonicity of the reservoir solution, drops were placed over a series of increasing sodium chloride concentrations (2.0–3.0 M sodium chloride in 50 mM increments). Single crystals suitable for X-ray diffraction data collection grew over 2.55 M sodium chloride at 4°C.

Phase diagram for the PEG-citrate system

The phase diagram was determined by the general approach described by Albertsson for aqueous two phase systems (34). In 15 ml conical centrifuge tubes (graduated at 0.1 ml increments), total systems containing PEG 600, sodium citrate, *myo*-inositol and HEPES at concentrations given in Table 1 were prepared by dilution of the appropriate stock solutions. To accelerate the separation of the two aqueous phases, the preparations were centrifuged at 1,500 *g* for 5 min. The total volume (V_0), as well as the volumes of upper (V_U) and lower phases (V_L) were read directly from the graduated centrifuge tubes (see Table 1). All procedures were performed at room temperature. The concentrations of PEG 600, sodium citrate and *myo*-inositol were determined by NMR on a Nicolet QE-300. Samples consisted of an aliquot of the phase to be analyzed plus $^1/_7$ the volume of 40% sodium benzoate (to give a final concentration of 5% sodium benzoate in each sample, providing an internal standard for concentration). NMR measurements were on 20 μl of sample combined with 0.4 ml of D_2O. The concentrations of PEG 600, sodium citrate and *myo*-inositol in each phase were calculated from the peak area relative to the sodium benzoate standard, the concentration of the component in the total system, and the measured volumes of the phases. For example, the concentration of a component in the lower phase is given by:

$$C_L = \frac{A_L V_0 C_0}{A_U V_U + A_L V_L} \quad (1)$$

where C_L and C_0 are concentrations of PEG 600, sodium citrate or inositol in the lower phase and the total system, respectively; V_L, V_U, and V_0 refer to the respective volumes of lower and upper phase and of the total system. The relative NMR peak areas of the component for which the concentration is to be calculated are given by A_L (lower phase) and A_U (upper phase).

Protein distribution between the PEG-rich and sodium citrate-rich phases

In a typical experiment, the buffer of the purified protein at 20.6 mg/ml was exchanged for 93 mM HEPES, pH 7.9 by repeated ultrafiltration (Centricon-10) and the protein concentration was adjusted to 16.3 mg/ml. The concentration of PI-PLC was determined spectrophotometrically as follows. The amino acid sequence of the mature PI-PLC protein from *B. cereus*, deduced from the nucleotide sequence of its coding region (35), was used to calculate the molar extinction coefficient by the method of Gill and von Hippel (36). The calculated value is $E^{0.1\%}_{280\,nm} = 1.83$. To provide a linear relation of PI-PLC concentration and absorbance at 280 nm, protein dilutions giving an $A_{280} < 0.6$ were used. Small volumes (160 μl) of total systems containing ¼ or ⅛ volume of 16.3 mg/ml PI-PLC were prepared in 0.65 ml microcentrifuge tubes. After brief vortexing to mix the components, complete phase separation was obtained after centrifugation at 12,000 *g* for 5 min. Volumes were determined by comparison to standard volumes in identical tubes. All procedures were performed at room temperature. The phases were removed and diluted 1:40 (upper phase) or 1:20 (lower phase) in water for measuring absorbance at 280 nm. The blanks for the spectrophotometer measurements were 1:40 or 1:20 dilutions of upper and lower phase from total systems without PI-PLC but otherwise identical.

X-ray diffraction

X-rays were generated from a Rigaku RU200 rotating copper anode source and CuKα (1.54 Å) radiation selected with a graphite monochromator. We examined diffraction and obtained screened precession photographs on Kodak direct exposure x-ray film DEF-5. Three-dimensional data were collected on a Xuong–Hamlin area detector (37).

RESULTS AND DISCUSSION

Hexagonal crystals of *B. cereus* PI-PLC

Small hexagonal crystals were obtained using PEG 8000 as the precipitant (Fig. 1). The largest crystals we observed were on the order of 0.12 mm × 0.12 mm × 0.35 mm. The crystals were mounted with their long axes perpendicular to the x-ray beam. A series of still photographs at various rotations about this axis show equivalent zones at 60° intervals. These zones are interspersed with another set of zones, 30° away. Both zones display *mm* symmetry, as seen on screened precession photographs. Only hexagonal space groups have such equivalent zones, axially spaced at 60°, with *mm* symmetry.

The major zone (*h0l*) was identified based on its more closely spaced layer lines, relative to the diagonal zone. The two zones have a common row of reflections, related to the axis of rotation between them, which only shows

TABLE 1 **Phase compositions for the aqueous two-phase systems containing PEG 600 and sodium citrate**

	Total system*‡			Upper phase§			Lower phase§		
	C_0		V_0	C_U		V_U	C_L		V_L
#	PEG 600 % (vol/vol)	Na citrate [M]	[ml]	PEG 600 % (vol/vol)	Na citrate [M]	[ml]	PEG 600 % (vol/vol)	Na citrate [M]	[ml]
a	40.00	0.43	10.2	51.58	0.05	7.9	0.22	1.72	2.3
b	37.30	0.40	10.9	48.15	0.08	8.8	0.74	1.49	2.5
c	35.00	0.38	11.8	44.15	0.11	9.3	0.95	1.36	2.5
d	31.10	0.33	13.3	36.18	0.19	11.3	2.40	1.12	2.0

* The composition of a total system states the concentration of all components in this preparation regardless of their distribution between the phases. All systems were prepared and analyzed at room temperature (23°C).
‡ The total systems also contained HEPES (50 mM) and *myo*-inositol (71 mM in *a*, 67 mM in *b*, 63 mM in *c*, and 56 mM in *d*). Additional data were recorded at constant *myo*-inositol (50 mM) concentration. The phase diagram was the same within experimental error.
§ The concentrations of PEG 600 and Na citrate in upper and lower phases were determined using NMR as described under Materials and Methods.

every sixth reflection, compared to neighboring rows. This row suggests a 6_1-screw operator along the *c* axis.

In the *hk0* photograph of the diffraction pattern, twelve symmetry mates are present for each reflection. This can only occur in our hexagonal space group if there are 2-fold axes of symmetry perpendicular to the 6-fold screw axis. We therefore assign the space group to be $P6_122$ (or the enantiomorphic space group, $P6_522$). This space group has twelve asymmetric units per unit cell.

We determined cell constants from an *h0l* precession photograph. The distance between reflections on the *h00* layer line indicates the cell parameters $a = b = 133$ Å. From the distance between $l = 6n$ reflections on the *00l* layer, *c* is calculated to be 231 Å. The unit cell volume (V) is $V = a^2c \sin 60° = 3.54 \times 10^6$ Å^3 or 295×10^3 Å^3 per asymmetric unit. To determine the most likely number of PI-PLC monomers in each asymmetric unit we assumed a crystal packing parameter of 2.15 Å^3/Dalton. This is the most commonly observed value in a survey of solved protein structures reported by Matthews (38). The resulting number of 35 kD proteins that can be accommodated in the asymmetric unit is 3.9. Thus, there are probably 4 PI-PLC monomers in each asymmetric unit of the hexagonal unit cell (2–5 are possibilities).

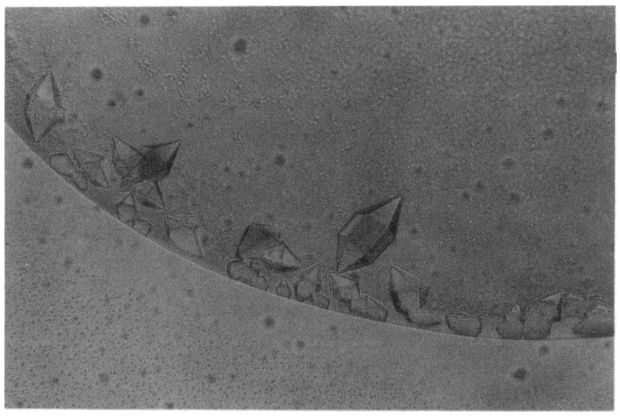

FIGURE 1 Light microscope photograph of hexagonal crystals of *B. cereus* PI-PLC. The hanging drop was prepared from 2 μl to 3 μl of about 8 mg/ml PI-PLC in distilled water, added to an equal amount of a precipitant solution containing 0.1 M ammonium sulfate and 15% (wt/vol) PEG 8000, pH 6.3. The drop was suspended over a 1 ml reservoir of the precipitant solution at room temperature. The largest crystal is approximately 0.05 × 0.1 mm.

Phase diagram for the PEG 600–sodium citrate system and partitioning of PI-PLC in the two phases

In our experience, orthorhombic PI-PLC crystals can be grown in PEG 600 and sodium citrate containing precipitant solution after phase separation occurs in the hanging drop, following partial dehydration of the hanging drop (usually >50%). Polyethylene glycols with other polymers, or certain combinations of water-soluble polymers and salt, cause separation into two aqueous phases, depending on the concentration of solutes. Although polyethylene glycols are frequently employed as precipitating reagents in protein crystallization studies (32, 39), these phase separations are rarely explored in detail. However, in the field of industrial-scale bioseparations, there is an extensive literature on aqueous two-phase systems based on two water soluble polymers, for example PEG and dextran (34, 40). These polymers, or certain combinations of water soluble polymers and salts, cause a separation into two aqueous phases. Proteins and other biological macromolecules added to these systems partition unequally between the two phases, and this partition provides the basis for protein isolation. In one study particularly relevant to the present work, Vernau and Kula (41) examined a series of aqueous two-phase systems resulting from mixtures of PEG 400 to 20,000 and sodium citrate. Their goal was to develop a system for extracting enzymes from cell homogenates based on biodegradable citrates. During the course of their work, Vernau and Kula established that PEG and sodium ci-

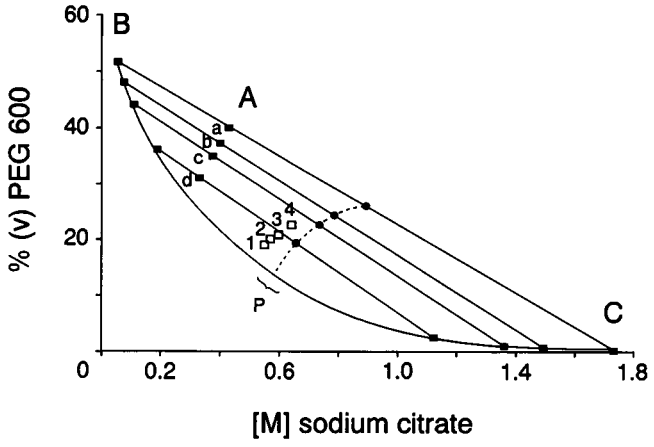

FIGURE 2 Phase diagram for the PEG 600–sodium citrate system at room temperature (23°C). The concentrations of the system components were selected to match those of the actual orthorhombic crystal growing solutions. (*A*) Total PEG 600 and sodium citrate concentrations for the four systems (*a–d*) of Table 1. (*B*, *C*) Nodes of the tie lines corresponding to compositions of the upper and lower phases, respectively. Also plotted on this phase diagram are the total compositions of four other systems (1–4, *open squares*) that additionally contained PI-PLC and were used to measure the partitioning of the protein (see Table 2). (*P*) is an estimate of the critical point.

trate will form a two-phase system in the absence of any added protein, and that a range of proteins (e.g., leucine dehydrogenase, alanine dehydrogenase, R-oxynitrilase, alcohol dehydrogenase, and glucose-6-phosphate reductase) are concentrated in the upper PEG-rich phase. Since our conditions are different from those examined by Vernau and Kula, we have determined the appropriate phase diagram for the PEG 600–sodium citrate system. The aim is to provide a better understanding of the PI-PLC crystal growth conditions, and to provide a basis for minimizing complications (e.g., crystal imperfections and perforations arising from contact with multiple droplets of the second phase during crystal growth).

The phase diagram for the PEG 600–sodium citrate system is shown in Fig. 2. PEG 600 and sodium citrate are both quite soluble in water, yet the two compounds together are incompatible and cause a separation into two phases when present in sufficiently high concentrations. By convention, the component enriched in the top phase is plotted on the ordinate and the component concentrated in the bottom phase on the abscissa. Mixtures with compositions below the curved line (binodial) produce a single homogeneous phase, whereas above this line, phase separation occurs. In Fig. 2, the points *a–d* are the total compositions selected to generate the binodial. The straight lines are tie lines. The line passing through *a*, for example, connects the points on the binodial representing the compositions of the two phases in equilibrium with the system of total composition represented by *a*. Volumes and densities of the phases, concentration of their components and distances on the tie lines $\overline{\mathbf{AC}}$ and $\overline{\mathbf{AB}}$ are related by:

$$\frac{V_U d_U}{V_L d_L} = \frac{\overline{\mathbf{AC}}}{\overline{\mathbf{AB}}} = \frac{C_L - C_0}{C_0 - C_U} \qquad (2)$$

where volumes and concentrations are defined as in the Materials and Methods (we neglect the small differences in densities of the two phases, and take $d_U \simeq d_L$). *Myo*-inositol, detected in lower phase only, and HEPES, which was found evenly distributed between the phases, were omitted from Fig. 2, for clarity.

The phase diagram explains several observations regarding the growth conditions of the orthorhombic crystals. Initially, the hanging drop consists of one homogeneous phase, corresponding to points well below the binodial of Fig. 2 (e.g., 14% PEG 600 and 0.15 M sodium citrate). As vapor diffusion progresses, the concentrations of PEG 600 and sodium citrate increase, until a phase separation occurs. PI-PLC crystal growth appears to be supported only in the upper but not in the lower phase. The phase separation is a property of the PEG 600–sodium citrate system, and is not caused by the PI-PLC.

To examine the partitioning of *B. cereus* PI-PLC between the two aqueous phases, total systems were prepared analogous to those in the phase diagram (Fig. 2) except that PI-PLC was added. The results are tabulated in Table 2. We found a distinct preference of PI-PLC for the PEG-rich phase, with partition coefficients ($K = C_U/C_0$) that correlate with the concentration of PEG 600 in the upper phase (K values for systems 1–4 are $K_1 = 2.4$, $K_2 = 5.9$, $K_3 = 16.5$, $K_{3b} = 17.5$, $K_4 = 35.0$, respectively). Thus, one effect of the phase separation is to concentrate the protein in the upper phase.

These results are in agreement with the protein separation studies of Vernau and Kula (41). At first glance, they might appear to be at variance with a report by Alber et al., (42) that yeast triose phosphate isomerase is concentrated in the *bottom* phase of a PEG 4000–ammonium sulfate system. However, it is well known that changes in the ions present can cause shifts in equilibrium concentrations of protein and other components between the upper and lower phases (34). In fact, Vernau and Kula (41) make use of this fact in a second step of their protein purification protocol. They were able to shift the protein concentration from the top PEG-rich phase to the bottom phase by replacing sodium citrate with sodium chloride. Thus, our results are consistent with the available literature.

By preparing systems 1–4 (Table 2), but omitting PI-PLC or adding *myo*-inositol or both (i.e., adding protein and *myo*-inositol), and comparing the volumes of upper and lower phases to those of systems 1–4, we detected volume differences only for variations of system 1, and these were small. Considering that modifications of system 1 occur nearest to the critical point P (see Fig. 2), the point where the property of a two phase system is most sensitive to variation in its composition (34), these

TABLE 2 **Distribution of *B. cereus* PI-PLC between the PEG-rich (upper) phase and the sodium citrate-rich (lower) phase**

	Total system*‡				Upper phase		Lower phase	
	C_0			V_0	C_U	V_U	C_L	V_L
#	PEG 600 % (vol/vol)	Na citrate pH 7.3 [M]	PI-PLC [mg/ml]§	[μl]‖	PI-PLC [mg/ml]¶	[μl]‖	PI-PLC [mg/ml]¶	[μl]‖
1	19.3	0.55	4.1	160	5.1	105	2.1	55
2	20.2	0.57	4.1	160	5.9	100	1.0	60
3	21.0	0.60	4.1	160	6.6	90	0.4	70
3b**	21.0	0.60	2.0	160	3.5	90	0.2	70
4	22.7	0.64	2.0	160	3.5	90	0.1	70

* see annotation Table 1.

‡ The total systems further contained 23.2 mM HEPES.

§ 16.3 mg/ml of PI-PLC in 93 mM HEPES, pH 7.9, was added to the systems (1–4) to give the indicated PI-PLC concentrations. In (3*b*) and (4), the buffer concentration was adjusted by adding the appropriate volume of 93 mM HEPES. At higher concentrations of PEG 600 and Na citrate protein precipitation was observed at 4.1 mg/ml, therefore, 2.0 mg/ml PI-PLC were used.

‖ Volume of total system (1–4) prepared (V_0), and volumes of upper (V_U) and lower (V_L) phases measured after phase-separation.

¶ The concentration of PI-PLC in the upper and lower phases was determined spectrophotometrically (see Materials and Methods section).

** System (3*b*) also contained 54.5 mM *myo*-inositol.

small differences are not surprising. We conclude that additives (PI-PLC and or *myo*-inositol) at concentrations used here cause only minor changes in the phase diagram. Therefore, tie lines of systems 2–4 can be projected into the phase diagram and the PEG 600 and sodium citrate concentrations of upper and lower phases deduced. Furthermore, we find addition of *myo*-inositol to be without influence on the partitioning of PI-PLC between upper and lower phases (Table 2, 3b). The presence of *myo*-inositol is not required for crystallization of PI-PLC as shown from our initial precipitant solution without *myo*-inositol. However, we find PI-PLC crystals formed in the presence of *myo*-inositol to be somewhat larger in size. The influence of *myo*-inositol on crystal growth might be via association with PI-PLC, for which we have indirect evidence from studies showing a weak inhibitory effect of *myo*-inositol on PI-PLC activity (43). However, any influence of *myo*-inositol is puzzling, since it partitions primarily to the lower phase.

Applying this analysis of the PEG 600-sodium citrate two phase system and partitioning of PI-PLC between the phases to crystal growth, we then asked if it is possible to grow crystals using precipitant solution composed of upper phase only. A single phase system from which protein can crystallize would be useful when defined changes to the precipitant are to be made (e.g., addition of cofactors or inhibitors) to avoid problems arising from unequal partitioning of additives between the phases. In preliminary experiments, we prepared several total systems consisting of PEG 600, sodium citrate, *myo*-inositol and 50 mM HEPES, pH 7.9, and removed the upper phase. Adding these solutions to an equal volume of protein solutions, we were able to grow orthorhombic crystals of PI-PLC at 4°C by the vapor diffusion technique. The crystals obtained were comparable to those of Fig. 3. From the phase diagram, and assuming vapor diffusion equilibrium with the well solution, we estimate the hanging drop contained between 36% PEG 600 and 0.19 M sodium citrate to 42% PEG 600 and 0.13 M sodium citrate. These results indicate that factors inherent in the process of phase separation *per se,* such as the presence of an interface or the gradual removal of citrate, are not essential for crystal growth.

Orthorhombic crystals of *B. cereus* PI-PLC

Representative crystals of the orthorhombic form of *B. cereus* PI-PLC are shown in Fig. 3. These crystals are somewhat larger and more easily obtained than the hex-

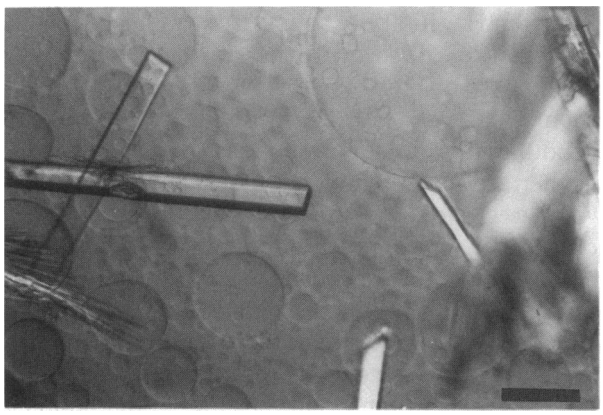

FIGURE 3 Light microscope photograph of orthorhombic crystals of *B. cereus* PI-PLC. In the background can be seen the droplets of a second phase. From the phase diagram and from PI-PLC partitioning between phases, this is identified as the sodium citrate-rich phase. The hanging drop was prepared from 7.5 μl of 9 mg/ml PI-PLC in 20 mM HEPES, pH 7.9, and 7.5 μl of 28% (vol/vol) PEG 600, 0.3 M sodium citrate, 50 mM *myo*-inositol. The drop was suspended over a 1 ml reservoir of 2.6 M NaCl at 4°C. The length of the bar is 0.2 mm.

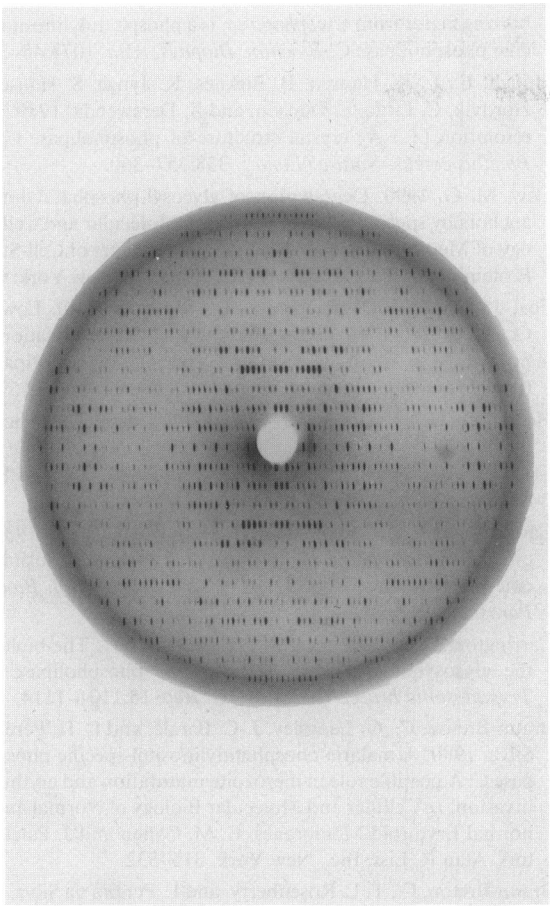

FIGURE 4 X-ray diffraction pattern of an orthorhombic crystal of *B. cereus* PI-PLC. 12° precession photograph of the *h0l* zone (*h* vertical, *l* horizontal).

agonal crystals of PI-PLC, typically reaching dimensions of about 0.05 mm × 0.1 mm × 1.0 mm. The orthorhombic crystals diffract surprisingly well for their relatively small size. We routinely obtain 12° screened precession photos in 24 hours.

By aligning the long axis of the brick-shaped crystals perpendicular to the beam and taking still x-ray photographs, we found two principal zones. These are related to each other by a 90° rotation about the crystal's long axis. A third principal zone is obvious when the crystal is oriented with its long axis parallel to the beam. We determined the cell constants and space group of these crystals from screened precession photographs of the three major zones. All three zones (*hk0*, *h0l*, and *0kl*) have *mm* symmetry and a common set of missing reflections. In the central horizontal and vertical rows, only alternate reflections are present. In the case of the *h0l* picture (see Fig. 4), these reflections are $h = 2n$ on the *h00* axis and $l = 2n$ on the *00l* axis. Only $k = 2n$ reflections are present on the *0k0* axis as judged from the *0kl* and *hk0* photographs.

The spacings between layer lines on these pictures were measured by hand and indicate constants of $a = 45$ Å, $b = 46$ Å, $c = 160$ Å. These unequal perpendicular cell axes are consistent with an orthorhombic unit cell. The systematic absences and *mm* symmetry seen on all three principal axes are consistent with space group $P2_12_12_1$. This space group has four asymmetric units per unit cell. The volume (V) of the orthorhombic unit cell is $V = abc = 3.31 \times 10^5$ Å^3, and thus the volume of each of the four asymmetric units is 82.8×10^3 Å^3. Assuming one monomer of PI-PLC (35 kD) per asymmetric unit, the molecular volume (V_m) is 2.38 Å^3/Dalton. This value is near the most common observed value of the packing parameter for known protein structures (38). Two monomers per unit cell would be highly unlikely because the corresponding V_m (1.19 Å^3/D) is well below the lowest observed value of this distribution.

X-ray diffraction from orthorhombic PI-PLC crystals extends to 2.5 Å resolution on our multi-wire area detector. In 48 hours, we collected the 20 Å–2.8 Å data summarized in Table 3. The statistics show a high completeness and redundancy. Between 20 Å and 3 Å, 91% of the independent reflections were measured, with each being measured an average of 3.5 times. The final R-factor of 0.046 indicates that data can be collected reliably to at least 2.8 Å. We intend to pursue the three-dimensional structure determination of *B. cereus* PI-PLC using the standard technique of multiple isomorphous replacement, and the search for suitable heavy atom derivatives is under way.

CONCLUSIONS

Two crystal forms of *B. cereus* PI-PLC are reported. This is evidently the first member of the large class of PI-specific phospholipase C enzymes to be crystallized. Small hexagonal crystals were grown from a single phase solution with PEG 8000 as the precipitating agent. Orthorhombic crystals were obtained from a more complex two phase system utilizing low molecular weight PEG (600 D) and sodium citrate. In order to provide a rational basis for understanding the crystallization process, the phase diagram was determined for the PEG 600 so-

TABLE 3 **Data collection for the orthorhombic form of *B. cereus* PI-PLC**

Resolution range (Å)	Number of unique reflections	Percentage of data	Average redundancy	R-factor*
∞–4.72	1864	94.4%	4.72	0.031
4.72–3.75	1718	94.3%	3.76	0.039
3.75–3.27	1656	92.2%	3.09	0.063
3.27–2.97	1646	91.0%	2.67	0.101
2.97–2.76	1057	59.5%	1.68	0.123
∞–2.76	7941	86.5%	3.34	0.046

* The R-factor (R-merge) was calculated as: *sum* (*abs* (*ave* − *obs*))/*sum* (*ave*), where *ave* is the average intensity of all the observed intensities (*obs*) for each reflection.

dium citrate system under the crystal growth conditions. Phase separation occurs spontaneously when PEG 600 and sodium citrate solutions are combined in the appropriate amounts, and it is not due to the PI-PLC. One effect of the phase separation, which occurs slowly in the hanging drop, is to concentrate PI-PLC in the upper PEG-rich phase, thus promoting crystallization. The phase diagram can be used to control the amount of the two phases present, and thus to minimize crystal imperfections caused by interference of droplets of the sodium citrate phase in the vicinity of crystals growing in the PEG-rich phase. Both crystal forms are suitable for crystallographic studies of *B. cereus* PI-PLC.

We wish to thank Drs. Brian W. Matthews, Dirk Heinz, Alistair Leigh, Steve Roderick, and Johannes J. Volwerk for useful discussions. We are pleased to acknowledge Renee Knoll and John A. Koke for protein isolation, and Karen Kallio, Jeannette Van, and Joan A. Wozniak for technical assistance. One of us (O. H. Griffith) wishes to thank his mentor, Dr. Harden M. McConnell, for the introduction to crystals and crystal symmetry many years ago at the California Institute of Technology, and to the staff of the 1990 Cold Spring Harbor Macromolecular Crystallography course for their help and encouragement.

This work was supported by the National Institutes of Health (GM25698 and GM42618) and by the National Science Foundation (DMB 8817438).

Received for publication 14 October 1992 and in final form 23 November 1992.

REFERENCES

1. Ikezawa, H., and R. Taguchi. 1981. Phosphatidylinositol-specific phospholipase C from *Bacillus cereus* and *Bacillus thuringiensis. Methods Enymol.* 71:731–741.
2. Griffith, O. H., J. J. Volwerk, and A. Kuppe. 1991. Phosphatidylinositol-specific phospholipases C from *Bacillus cereus* and *Bacillus thuringiensis. Methods Enzymol.* 197:493–502.
3. Henner, D. J., M. Yang, E. Chen, R. Hellmiss, H. Rodriguez, and M. G. Low. 1988. Sequence of the *Bacillus thuringiensis* phosphatidylinositol-specific phospholipase C. *Nucl. Acids Res.* 16:10383.
4. Lechner, M., T. Kupke, S. Stefanovic, and F. Götz. 1989. Molecular characterization and sequence of phosphatidylinositol-specific phospholipase C of *Bacillus thuringiensis. Mol. Microbiol.* 3:621–626.
5. Low, M. G. 1981. Phosphatidylinositol-specific phospholipase C from *Staphylococcus aureus. Methods Enzymol. (Lipids, Pt. C).* 71:741–746.
6. Mengaud, J., C. Braun-Breton, and P. Cossart. 1991. Identification of phosphatidylinositol-specific phospholipase C activity in *Listeria monocytogenes:* a novel type of virulence factor? *Mol. Microbiol.* 5:367–372.
7. Leimeister-Wächter, M., E. Domann, and T. Chakraborty. 1991. Detection of a gene encoding a phosphatidylinositol-specific phospholipase C that is co-ordinately expressed with listeriolysin in *Listeria monocytogenes. Mol. Microbiol.* 5:361–366.
8. Portnoy, D. A., T. Chakraborty, W. Goebel, and P. Cossart. 1992. Molecular determinants of *Listeria monocytogenes* pathogenesis. *Infect. Immun.* 60:1263–1267.
9. Jäger, K., S. Stieger, and U. Brodbeck. 1991. Cholinesterase solubilizing factor from *Cytophaga* sp. is a phosphatidylinositol-specific phospholipase C. *Biochim. Biophys. Acta.* 1074:45–51.
10. Hough, E., L. K. Hansen, B. Birknes, K. Jynge, S. Hansen, A. Hordvik, C. Little, E. Dodson, and Z. Derewenda. 1989. High-resolution (1.5 Å) crystal structure of phospholipase C from *Bacillus cereus. Nature (Lond.).* 338:357–360.
11. Low, M. G. 1990. Degradation of glycosyl-phosphatidylinositol anchors by specific phospholipases. *In* Molecular and Cell Biology of Membrane Proteins. Glycolipid Anchors of Cell-Surface Proteins. A. J. Turner, editor. Ellis Horwood, New York. Ch. 2.
12. Fox, J. A., M. Duszenko, M. A. J. Ferguson, M. G. Low, and G. A. M. Cross. 1986. Purification and characterization of a novel glycan-phosphatidylinositol-specific phospholipase C from *Trypanosoma brucei. J. Biol. Chem.* 261:15767–15771.
13. Hereld, D., G. W. Hart, and P. T. Englund. 1988. cDNA encoding the glycosyl-phosphatidylinositol-specific phospholipase C of *Trypanosoma brucei. Proc. Natl. Acad. Sci. USA.* 85:8914–8918.
14. Carrington, M., R. Büelow, H. Reinke, and P. Overath. 1989. Sequence and expression of the glycosyl-phosphatidylinositol-specific phospholipase C of *Trypanosoma brucei. Mol. Biochem. Parasitol.* 33:289–296.
15. Carrington, M., D. Walters, and H. Webb. 1991. The biology of the glycosylphosphatidylinositol-specific phospholipase C of *Trypanosoma brucei. Cell Biol. Int. Rep.* 15:1101–1114.
16. Braun-Breton, C., G. Langsley, J.-C. Barale, and L. H. Pereira da Silva. 1990. A malaria phosphatidylinositol-specific phospholipase C: A possible role in merozoite maturation and erythrocyte invasion. *In* Cellular and Molecular Biology of Normal and Abnormal Erythroid Membranes. C. M. Cohen and J. Palek, editors. Alan R. Liss, Inc., New York. 315–332.
17. Braun-Breton, C., T. L. Rosenberry, and L. Pereira da Silva. 1988. Induction of the proteolytic activity of a membrane protein in *Plasmodium falciparum* by phosphatidyl inositol-specific phospholipase C. *Nature (Lond.)* 332:457–459.
18. Cubitt, A. B., and R. A. Firtel. 1992. Characterization of phospholipase activity in *Dictyostelium discoideum. Biochem. J.* 283:371–378.
19. Bloomquist, B. T., R. D. Shortridge, S. Schneuwly, M. Perdew, C. Montell, H. Steller, G. Rubin, and W. L. Pak. 1988. Isolation of a putative phospholipase C gene of Drosophila, *norpA,* and its role in phototransduction. *Cell.* 54:723–733.
20. Masai, I., and Y. Hotta. 1991. Genomic organization of a *Drosophila* phospholipase C *norpA,* and molecular lesions in two temperature-sensitive mutants. *J. Biochem.* 109:867–871.
21. Shortridge, R. D., J. Yoon, C. R. Lending, B. T. Bloomquist, M. H. Perdew, and W. L. Pak. 1991. A *Drosophila* phospholipase C gene that is expressed in the central nervous system. *J. Biol. Chem.* 266:12474–12480.
22. Waldo, G. L., A. J. Morris, D. G. Klapper, and T. K. Harden. 1991. Receptor- and G-protein-regulated 150-kD avian phospholipase C: Inhibition of enzyme activity by isoenzyme-specific antisera and nonidentity with mammalian phospholipase C isoenzymes established by immunoreactivity and peptide sequence. *Mol. Pharmacol.* 40:480–489.
23. Harden, T. K., A. J. Morris, G. L. Waldo, C. T. Downes, J. L. Boyer. 1991. Avian G-protein-regulated phospholipase C. *Biochem. Soc. Trans.* 19:342–346.
24. Rhee, S. G. and K. D. Choi. 1992. Regulation of inositol phospholipid-specific phospholipase C isozymes. *J. Biol. Chem.* 267:12393–12396.
25. Rhee, S. G., S. H. Ryu, K. Y. Lee, and K. S. Cho. 1991. Assays of phosphoinositide-specific phospholipase C and purification of isozymes from bovine brains. *Methods Enzymol.* 197:502–511.
26. Dennis, E. A., S. G. Rhee, M. M. Billah, and Y. A. Hannun. 1991.

Role of phospholipases in generating lipid second messengers in signal transduction. *FASEB (Fed. Am. Soc. Exp. Biol.) J.* 5:2068–2077.

27. Ting, A. E., and R. E. Pagano. 1990. Detection of a phosphatidylinositol-specific phospholipase C at the surface of Swiss 3T3 cells and its potential role in the regulation of cell growth. *J. Biol. Chem.* 265:5337–5340.
28. Volwerk, J. J., G. B. Birrell, K. K. Hedberg, and O. H. Griffith. 1992. A high level of cell surface phosphatidylinositol-specific phospholipase C activity is characteristic of growth-arrested 3T3 fibroblasts but not of transformed variants. *J. Cell. Physiol.* 151:613–622.
29. McMurray, W. C., and R. F. Irvine. 1988. Phosphatidylinositol 4,5-bisphosphate phosphodiesterase in higher plants. *Biochem. J.* 249:877–881.
30. Melin, P.-M., M. Sommarin, A. S. Sandelius, and B. Jergil. 1987. Identification of Ca^{2+}-stimulated polyphosphoinositide phospholipase C in isolated plant plasma membranes. *FEBS (Fed. Eur. Biochem. Soc.) Lett.* 223:87–91.
31. Koke, J. A., M. Yang, D. J. Henner, J. J. Volwerk, and O. H. Griffith. 1991. High-level expression in *Escherichia coli* and rapid purification of phosphatidylinositol-specific phospholipase C from *Bacillus cereus* and *Bacillus thuringiensis. Protein Expression and Purif.* 2:51–58.
32. McPherson, A. 1989. Preparation and Analysis of Protein Crystals, 2nd ed. Robert E. Krieger Publishing Co., Inc., Malabar, FL. Ch. 4.
33. Jancarik, J., and S.-H. Kim. 1991. Sparse matrix sampling: a screening method for crystallization of proteins. *J. Appl. Cryst.* 24:409–411.
34. Albertsson, P.-A. 1986. Partition of Cell Particles and Macromolecules. 3rd ed. John Wiley & Sons Inc., New York. Ch. 2.
35. Kuppe, A., L. M. Evans, D. A. McMillen, and O. H. Griffith. 1989. Phosphatidylinositol-specific phospholipase C of *Bacillus cereus:* Cloning, sequencing, and relationship to other phospholipases. *J. Bacteriol.* 171:6077–6083.
36. Gill, S. C., and P. H. von Hippel. 1989. Calculation of protein extinction coefficients from amino acid sequence data. *Anal. Biochem.* 182:319–326.
37. Xuong, N. H., C. Nielsen, R. Hamlin, and D. Anderson. 1985. Strategy for data collection from protein crystals using a multiwire counter area detector diffractometer. *J. Appl. Cryst.* 18:342–350.
38. Matthews, B. W. 1968. Solvent Content of Protein Crystals. *J. Mol. Biol.* 33:491–497.
39. Ducruix, A. and R. Giegé, editors. 1992. Crystallization of Nucleic Acids and Proteins. A Practical Approach. IRL Press at Oxford University Press, Oxford. 331 pp.
40. Hamel, J.-F. P., J. B. Hunter, and S. K. Sikdar, editors. 1990. Downstream Processing and Bioseparation: Recovery and Purification of Biological Products. ACS Symposium Series 419. American Chemical Society, Washington, DC. Ch. 1–4.
41. Vernau, J., and M.-R. Kula. 1990. Extraction of proteins from biological raw material using aqueous polyethylene glycol-citrate phase systems. *Biotechnol. Appl. Biochem.* 12:397–404.
42. Alber, T., F. C. Hartman, R. M. Johnson, G. A. Petsko, and D. Tsernoglou. 1981. Crystallization of yeast triose phosphate isomerase from polyethylene glycol. *J. Biol. Chem.* 256:1356–1361.
43. Shashidhar, M. S., J. J. Volwerk, J. F. W. Keana, and O. H. Griffith. 1990. Inhibition of phosphatidylinositol-specific phospholipase C by phosphonate substrate analogues. *Biochim. et Biophys. Acta.* 1042:410–412.